HETEROGENEOUS NUCLEATION IN A 2-D MODEL OF MARTENSITIC TRANSFORMATION WITH VOLUME CHANGES

WENWU CAO AND RAJEEV AHLUWALIA
Materials Research Laboratory, The Pennsylvania State University, University Park, Pennsylvania 16802

We study domain pattern formation in a 2-D square to rectangle martensitic transformation using a time-dependent Ginzburg-Landau model. The model is based on a free energy in terms of the deviatoric, bulk and shear components of the strain tensor. In this work, we include a coupling between the deviatoric and bulk strains that allows for volume changes of the unit cell. An effective free energy in terms of deviatoric strains is constructed by eliminating the bulk and shear strains subject to the elastic compatibility relations. Heterogeneous nucleation is studied by considering randomly distributed stress centers that represent crystal defects. Computer simulations of the model reveal that the stress centers nucleate product phase domains that grow only in finite size. Hence, there is always some retained parent phase at the end of the transformation.

1. Introduction

The microstructure of martensitic materials exhibits fascinating domain patterns. Typically, the product phase domains grow anisotropically and have low aspect ratio. Usually, the parent and product phases are found to coexist with a pattern of crisscross domains that are separated by intermediate austenite regions that failed to transform[1]. The martensite domains may themselves be internally twinned. Clearly, there is a need for theoretical models to explain the complex microstructure observed in real materials. Recently, the microstructure of these materials has been studied by simulation models based on the Landau-Ginzburg approach [2-4]. This is a very useful technique to study domain patterns, as one does not need to make *a priori* assumptions about the domain wall orientations. The microstructure is a consequence of the appropriate symmetry built into the free energy.

In this work, we are particularly interested in the "Proper Ferroelastic Martensitic Transformations". Here, the strain itself is the order parameter as the unit cell undergoes a shape change. A 3-D Landau-Ginzburg free energy for proper ferroelastic transformations was first proposed by Barsch and Krumhansl [5]. Recently, Shenoy and coworkers made a 2-D simulation for the square to rectangle transition and showed that the microstructure in these materials was a consequence of elastic compatibility requirement[3]. Here we use the elastic compatibility approach to study a square to rectangle transition, in which a coupling between bulk and deviatoric strain explicitly occurs in the free energy. This coupling corresponds to the volume changes associated with the unit cell. We show below that the simple coupling discussed above drastically influences the simulated microstructures.

Q.P. Sun (ed.), IUTAM Symposium on Mechanics of Martensitic Phase Transformation in Solids, 213–220.

2. Model

The model is based on a free energy functional in terms of the bulk strain $\phi_1 = (\eta_{xx} + \eta_{yy})/\sqrt{2}$, the deviatoric strain $\phi_2 = (\eta_{xx} - \eta_{yy})/\sqrt{2}$ and the shear strain $\phi_3 = \eta_{xy}$, where η_{ij} represents the component of the linearized strain tensor. The free-energy is given as

$$F = F_d[\phi_2] + F_h[\phi_1, \phi_3] + F_c[\phi_2, \phi_1], \tag{1}$$

where $F_d[\phi_2]$ is the free-energy contribution due to the dominant devatoric strains. The term $F_h[\phi_1, \phi_3]$ is the harmonic contribution due to bulk and shear strains and $F_c[\phi_1, \phi_2]$ is the coupling between bulk and deviatoric strain. The deviatoric contribution is given by

$$F_d[\phi_2] = \int d\vec{r}[f(\phi_2) + \frac{\gamma_1}{2}(\vec{\nabla}\phi_2)^2 + \frac{\gamma_2}{2}(\nabla^2\phi_2)^2], \tag{2}$$

where strain gradient energy contribution has also been included. Since the deviatoric mode is the dominant mode for the transition, a sixth order polynomial is chosen for the $f(\phi_2)$ to describe a first order phase transition. The harmonic free-energy due to bulk and shear strain is given as

$$F_h[\phi_1, \phi_3] = \int d\vec{r}[\frac{A_1}{2}{\phi_1}^2 + \frac{A_3}{2}{\phi_3}^2], \tag{3}$$

where, A_1 and A_3 are constants that can be obtained from the elastic constants of the material. The coupling term between bulk and deviatoric strain is given as

$$F_c[\phi_1, \phi_2] = \int d\vec{r}[A_{12}\phi_1{\phi_2}^2]. \tag{4}$$

We should also consider the fact that the strains ϕ_1, ϕ_2 and ϕ_3 are not independent but are linked by the elastic compatibility relations [6]. In terms of the strain variables, these relations are expressed as

$$\nabla^2\phi_1 - (\frac{\partial^2}{\partial x^2} - \frac{\partial^2}{\partial y^2})\phi_2 - \frac{\partial^2}{\partial x \partial y}\phi_3 = 0. \tag{5}$$

We now make use of an elimination procedure similar to the one first proposed by Kartha et. al [6]. In this approach, the bulk and shear strains are eliminated subject to the constraint expressed in Eqn. (5). For our model, the elimination procedure results in an

effective long-range interaction that replaces the terms $F_h[\phi_1,\phi_3]+F_c[\phi_1,\phi_2]$. The effective interaction is conveniently expressed in Fourier space as

$$F_{eff}=\int d\vec{k}C_1(\vec{k})|\phi_2(\vec{k})|^2+\int d\vec{k}C_2(\vec{k})|\Gamma(\vec{k})|^2+\int d\vec{k}C_3(\vec{k})\phi_2(-\vec{k})\Gamma(\vec{k}) \qquad (6)$$

where $\phi_2(\vec{k})$ and $\Gamma(\vec{k})$ are respectively the Fourier transforms of $\phi_2(\vec{r})$ and $\phi_2(\vec{r})^2$ and the kernels

$$C_1(\vec{k})=(1/2)(k_x^2-k_y^2)^2/[k^4/A_1+8k_x^2k_y^2/A_3] \qquad (7)$$

$$C_2(\vec{k})=-(A_{12}^2/2A_1A_3)(8k_x^2k_y^2)/[k^4/A_1+8k_x^2k_y^2/A_3] \qquad (8)$$

$$C_3(\vec{k})=(A_{12}/A_1)(k_x^2-k_y^2)(k_x^2+k_y^2)/[k^4/A_1+8k_x^2k_y^2/A_2] \qquad (9)$$

where, $k^4=(k_x^2+k_y^2)^2$.

After eliminating the bulk and the shear strain, we have a free energy only in terms of the deviatoric strain $\phi_2(\vec{r})$. To study the domain pattern formation, we study the time evolution of $\phi_2(\vec{r})$ using the time dependent Ginzburg-Landau formalism. The equation of motion is given as

$$\frac{\partial\phi_2(\vec{r})}{\partial t}=-L\frac{\delta F[\phi_2(\vec{r})]}{\delta\phi_2(\vec{r})} \qquad (10)$$

where L is kinetic coefficient and $F=F_d[\phi_2]+F_{eff}[\phi_2]$. We adopt a rescaling procedure of the free energy for the simulations, similar to the one discussed in [7] and accordingly use the polynomial

$$f(\phi_2)=\frac{\tau}{2}\phi_2(\vec{r})^2-\phi_2(\vec{r})^4+\frac{1}{2}\phi_2(\vec{r})^6-\sigma(\vec{r})\phi_2(\vec{r}) \qquad (11)$$

where τ is a rescaled temperature. All other variables in the effective free energy, such as A_1, A_3 and A_{12}, are also assumed to be rescaled. The term $\sigma(\vec{r})$ represents an inhomogeneous stress field that represents localized crystal defects [7]. We consider a configuration of randomly distributed defects with stress field given as

$$\sigma(\vec{r})=\sum_{j=1}^{N_d}\sigma_0(\vec{r}_j)\exp(-|\vec{r}-\vec{r}_j|^2). \qquad (12)$$

3. Simulations

We now describe our simulations of domain pattern formation using the above described model. The constants chosen for the local free energy are: $\tau = -0.1, \gamma_1 = 0.5, \gamma_2 = 0.01$. The amplitude of the local stress field $\sigma_0(\vec{r}_j)$ is chosen as being uniformly distributed in the interval [-0.6,0.6] and the total number of defects Nd is 288, which is 2% of the total grids. The parameters $A_1 = 1$ and $A_3 = 2$. For the coupling constant, we consider two cases below to illustrate the associated microstructure pattern formation:

Case A: This corresponds to $A_{12} = 1.2.$, where the transformed regions undergo a decrease in volume at the level of homogeneous elasticity. We discretize equation (10) on a 128×128 grid. Starting from small amplitude initial conditions, corresponding to an austenite phase, equation (10) is solved at each discrete grid point at each time step. Figure 1. shows the time evolution of the domain patterns obtained by simulating equation (10) for t = 40 (the time is assumed to be rescaled by the kinetic coefficient L) steps. In the snapshot corresponding to t=3, we can observe nucleation of product phase domains from the localized defects. Here the gray background corresponds to the Austenite phase while the dark and light regions represent the two variants of the martensitic phase. Notice that initially the domains grow very fast along [11] or $[\bar{1}1]$directions with little sidewise growth. The onward growth is usually stopped by collision with other growing domains. In the very late stages, there is more sidewise motion and eventually the final pattern consists of crisscross martensite domains that partition the austenite matrix. Thus, there is retained austenite at the end of the transformation. These domain patterns are similar to the ones simulated in the phenomenological model in [4]. However, the martensite domains are not internally twinned due to the over damped model used by us. Inclusion of inertial effects in this model may induce internal twinning [8].

Case B: Here we consider the case $A_{12} = -1.2$, which corresponds to the situation where the volume of the unit cell increases at the level of homogeneous free energy. Figure 2 shows the domain pattern evolution for this case. This case appears to be different than the one shown in figure 1. Here the nuclei give rise to islands of the product phase that grow along the 45° directions. The growing domains may coalesce with adjacent domains. The final microstructure can be seen in the snapshot corresponding to t=40. It is clear that the nature of the simulated domain patterns is quite different for this case. However, even for this case, there is retained austenite at the end of the transformation. This difference in patterns is likely due the long-range kernel $C_3(\vec{k})$ that depends linearly on A_{12}. In figure 3, we display the time dependence of the volume fraction of the martensite phase for both the cases discussed above. We can clear see that after a small incubation period, there is a sudden increase in the volume fraction. This corresponds to the initial nucleation stage. Thereafter, the volume fraction appears to saturate. Notice that the saturation value is lower for the case with negative A_{12}.

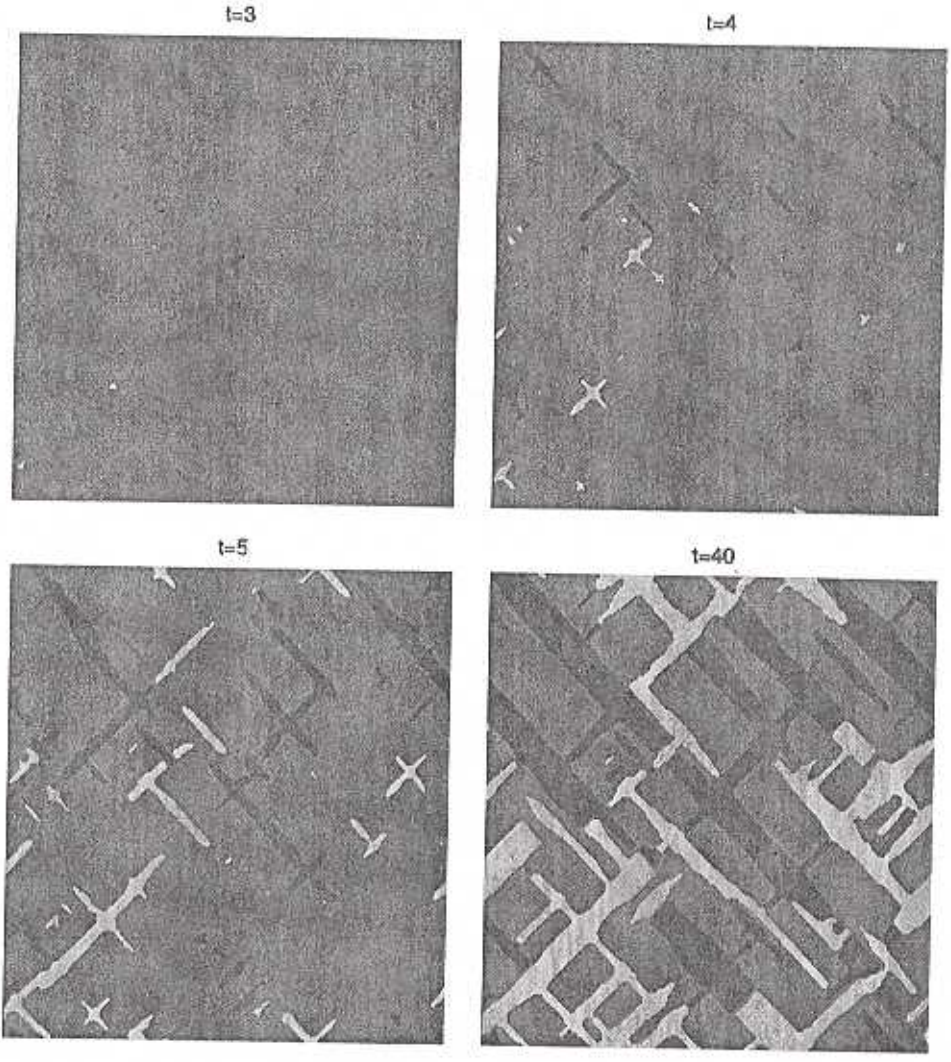

Figure 1. Domain pattern evolution for $A_{12} = 1.2$, case. The light and dark colors represent the two variants of the transformed martensite phase while the gray background represents the austenite phase.

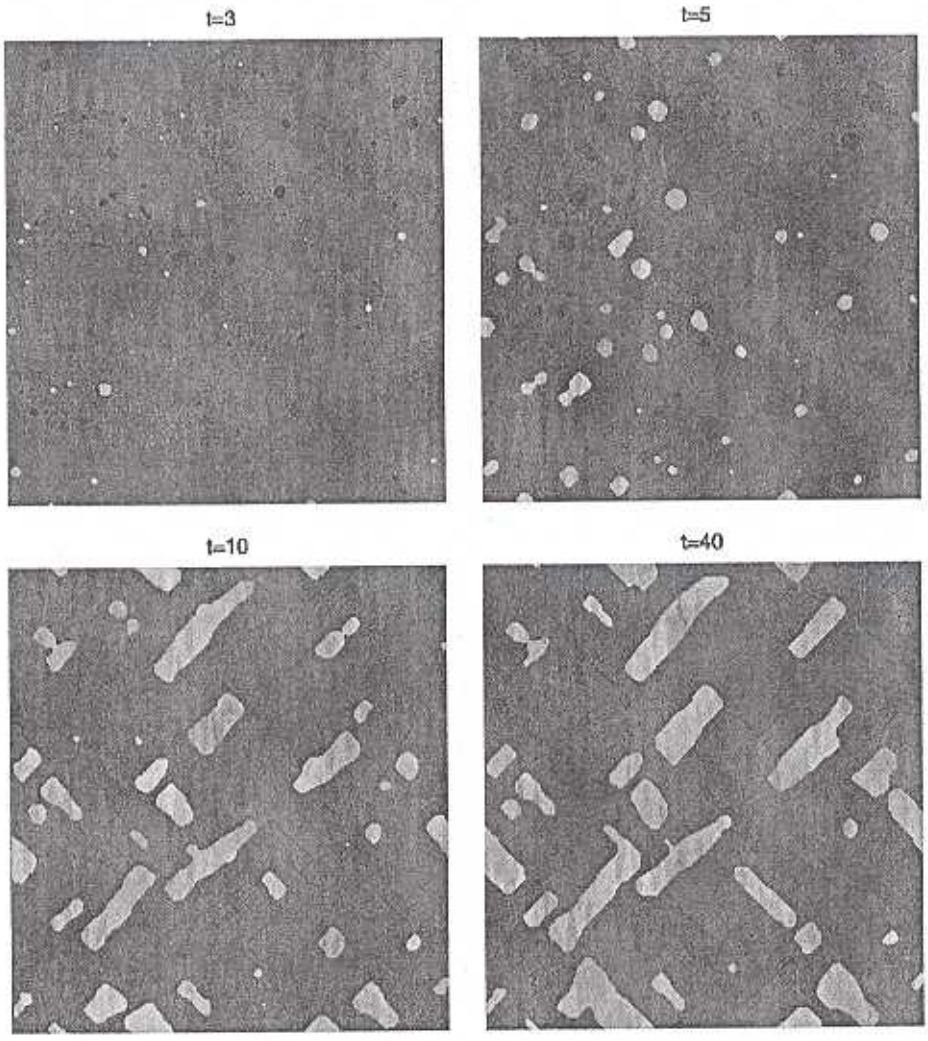

Figure 2. Pattern evolution for the case $A_{12} = -1.2$, . Color scheme is the same as that of figure 1.

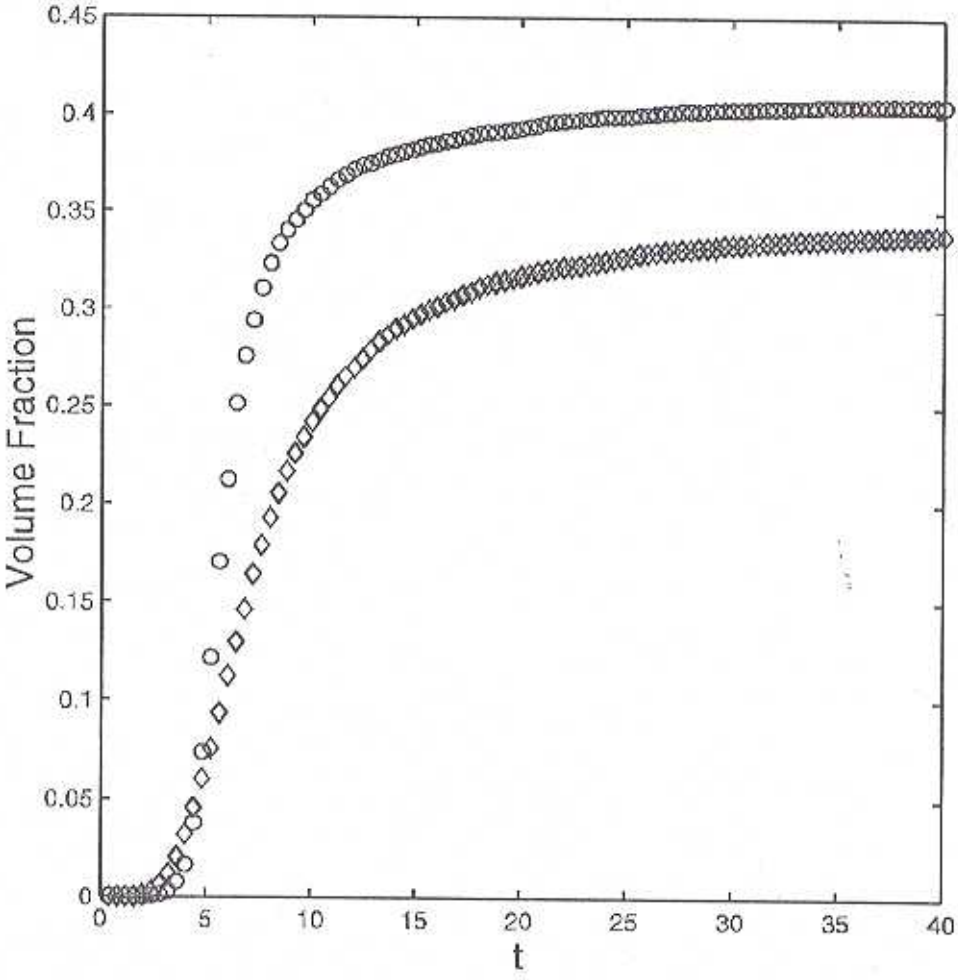

Figure 3. Time evolution of the volume fraction of martensite phase. Circles represent $A_{12} = 1.2$. and diamonds represent $A_{12} = -1.2$..

4. Discussion

We have made a computer simulation study of domain pattern formation in martensites based on a time-dependent Ginzburg-Landau model. It is found that inclusion of volume changes in the theory influences the domain patterns considerably. By including the coupling between bulk and deviatoric strains, we have shown that there is always some untransformed austenite left at the end of the transformation. This should be contrasted with case studied in [3] corresponding to $A_{12}=0$ where twin patterns were observed without any residual Austenite. Of course, even for $A_{12}\neq 0$, at low enough temperature we expect that there would be no more austenite since the driving force would be high enough.

5. References

1. Olson G. B. and Owen W. S., Editors, (1992) *Martensite*, ASM International.
2. Wang, Y. and Khachaturyan, A.G. (1997) Three-dimensional field model and computer modeling of martensitic transformations, *Acta Materialia* **45**,759-773.
3. Shenoy, S.R., Lookman ,T., Saxena A. and Bishop, A.R. (1999) Martensitic textures: Multiscale consequences of Elastic Compatibility, *Phys.Rev. B* **60**, R12537-R12541.
4. Ahluwalia ,R. and Ananthakrishna G. (2001) Power-Law Statistics of Avalanches in a Martensitic Transformation, *Phys. Rev. Lett.* **86**, 4076-4079.
5. Barsch, G.R. and Krumhansl, J. A. (1984) Twin Boundaries in Ferroelastic Media without Interface Dislocations, *Phys. Rev. Lett* **53**, 1069-1072
6. Kartha ,S., Krumansl, J.A., Sethna, J.P., Wickham,L. (1995) Disorder driven Pretransitional Tweed Patterns in Martensitic Transformations, *Phys. Rev. B* **52**,803-822.
7. Cao, W.W. and Krumhansl, J. A. (1990) Defect-Induced Heterogeneous Transformations and Thermal Growth in Athermal Martensite, *Phys. Rev. B* **41**, 11319-11327.
8. Bales, G.S. and Gooding, R.J. (1991) Interfacial Dynamics at a First-Order Phase Transition involving Strain-Dynamic Twin formation, *Phys. Rev. Lett.* **67**,3412-3415.